Article

RNA-seq Analysis of Solanesol Biosynthesis Genes in *Nicotiana tabacum*

Ning Yan [1], Hongbo Zhang [1], Zhongfeng Zhang [1], John Shi [2], Michael P. Timko [3], Yongmei Du [1], Xinmin Liu [1] and Yanhua Liu [1,*]

[1] Tobacco Research Institute of Chinese Academy of Agricultural Sciences, Qingdao 266101, China; yanning@caas.cn (N.Y.); zhanghongbo@caas.cn (H.Z.); zhangzhongfeng@caas.cn (Z.Z.); duyongmei@caas.cn (Y.D.); liuxinmin@caas.cn (X.L.)

[2] Guelph Food Research Center, Agriculture and Agri-Food Canada, Guelph, ON N1G 5C9, Canada; john.shi@agr.gc.ca

[3] Department of Biology, University of Virginia, Charlottesville, VA 22904, USA; mpt9g@virginia.edu

* Correspondence: 13646810352@163.com; Tel.: +86-532-8870-1035

Abstract: Solanesol is a noncyclic terpene alcohol composed of nine isoprene units and it mainly accumulates in solanaceous plants, especially tobacco (*Nicotiana tabacum* L.). Here, RNA-seq analyses of tobacco leaves, stems, and roots were used to identify solanesol biosynthesis genes. Six 1-deoxy-D-xylulose 5-phosphate synthase, two 1-deoxy-D-xylulose 5-phosphate reductoisomerase, two 2-*C*-methyl-D-erythritol 4-phosphate cytidylyltransferase, four 4-diphosphocytidyl-2-*C*-methyl-D-erythritol kinase, two 2-*C*-methyl-D-erythritol 2,4-cyclodiphosphate synthase, four 1-hydroxy-2-methyl-2-(*E*)-butenyl 4-diphosphate synthase, two 1-hydroxy-2-methyl-2-(*E*)-butenyl 4-diphosphate reductase, six isopentenyl diphosphate isomerase, and two solanesyl diphosphate synthase (*SPS*) genes were identified to be involved in solanesol biosynthesis. Furthermore, the two *N. tabacum* SPS (NtSPS1 and NtSPS2), which had two conserved aspartate-rich DDxxD domains, were highly homologous with SPS enzymes from other solanaceous plant species. In addition, the solanesol contents of three organs, and leaves from four growing stages, corresponded with the distribution of chlorophyll. Our findings provide a comprehensive evaluation of the correlation between the expression of different biosynthetic genes and the accumulation of solanesol in tobacco.

Keywords: *Nicotiana tabacum*; solanesol; RNA-seq; solanesyl diphosphate synthase; gene expression; chlorophyll

1. Introduction

Solanesol is a noncyclic terpene alcohol synthesized by the condensation of nine isoprene units, and this molecule is a precursor in the synthesis of ubiquinones and anti-cancer drugs, such as coenzyme Q_{10}, vitamin K_2, and *N*-solanesyl-*N*, *N*′-bis(3,4-dimethoxybenzyl) ethylenediamine (SDB) [1–3]. Coenzyme Q_{10} has anti-oxidant and anti-aging properties and is reported to strengthen the body's immune system and cardiovascular function, improve brain health, and moderate blood lipids. As a result, it has potential for the treatment of migraines, neurodegenerative diseases, hypertension, and cardiovascular diseases [2–5], and it is also being used as a dietary supplement by patients with type 2 diabetes [6]. Vitamin K_2 promotes bone formation and mineralization, inhibits bone resorption, has preventive and therapeutic effects on osteoporosis, promotes blood coagulation, and improves arterial stiffness [7]. Meanwhile, SDB can overcome several types of drug resistance in tumours mediated by P-proteins and plays a synergistic role with certain antitumor drugs [8,9]. Yao et al. [10] also reported that solanesol could protect human hepatic L02 cells from ethanol-induced oxidative injury *via* upregulation of *HO-1* and *Hsp70* expression. Thus, the medical benefits of solanesol and its derivatives are well established.

However, as a long-chain polyisoprenoid alcohol, solanesol is difficult to synthesize *de novo* [11], and the primary source of solanesol is *via* extraction from plants, particularly tobacco leaves [3,12]. The molecule was first isolated from tobacco (*Nicotiana tabacum* L.) in 1956 and has subsequently been reported to occur in other solanaceous plants, including tomatoes, potatoes, eggplants, and peppers [1,3,12]. Solanesol exists in both free and ester-bound states in solanaceous plants [3,12]. Zhou and Liu [13] reported that the solanesol content of tobacco leaves from 16 regions of China ranged from 0.4 to 1.7 %, and to identify solanesol-rich tobacco varieties, we found that the solanesol content of leaves from 93 tobacco varieties ranged from 1.78 to 3.60 % [3]. Furthermore, pathogen infection, drought, shade, long-wavelength and extended irradiation, and treatment with rare earth elements have been shown to influence the solanesol content of tobacco leaves [3,12].

Solanesol biosynthesis occurs in the plastids of higher plants *via* the 2-*C*-methyl-D-erythritol 4-phosphate (MEP) pathway [3,12,14], and the key enzymes of solanesol biosynthesis include 1-deoxy-D-xylulose 5-phosphate synthase (DXS), 1-deoxy-D-xylulose 5-phosphate reductoisomerase (DXR), 2-*C*-methyl-D-erythritol 4-phosphate cytidylyltransferase (IspD), 4-diphosphocytidyl-2-*C*-methyl-D-erythritol kinase (IspE), 2-*C*-methyl-D-erythritol 2,4-cyclodiphosphate synthase (IspF), 1-hydroxy-2-methyl-2-(*E*)-butenyl 4-diphosphate synthase (IspG), 1-hydroxy-2-methyl-2-(*E*)-butenyl 4-diphosphate reductase (IspH), isopentenyl diphosphate isomerase (IPI), and solanesyl diphosphate synthase (SPS) (Figure 1) [3,12]. However, although Yan et al. [3] summarized the metabolic pathway and key enzymes of solanesol biosynthesis, few studies have reported the cloning and expression analysis of related genes in tobacco.

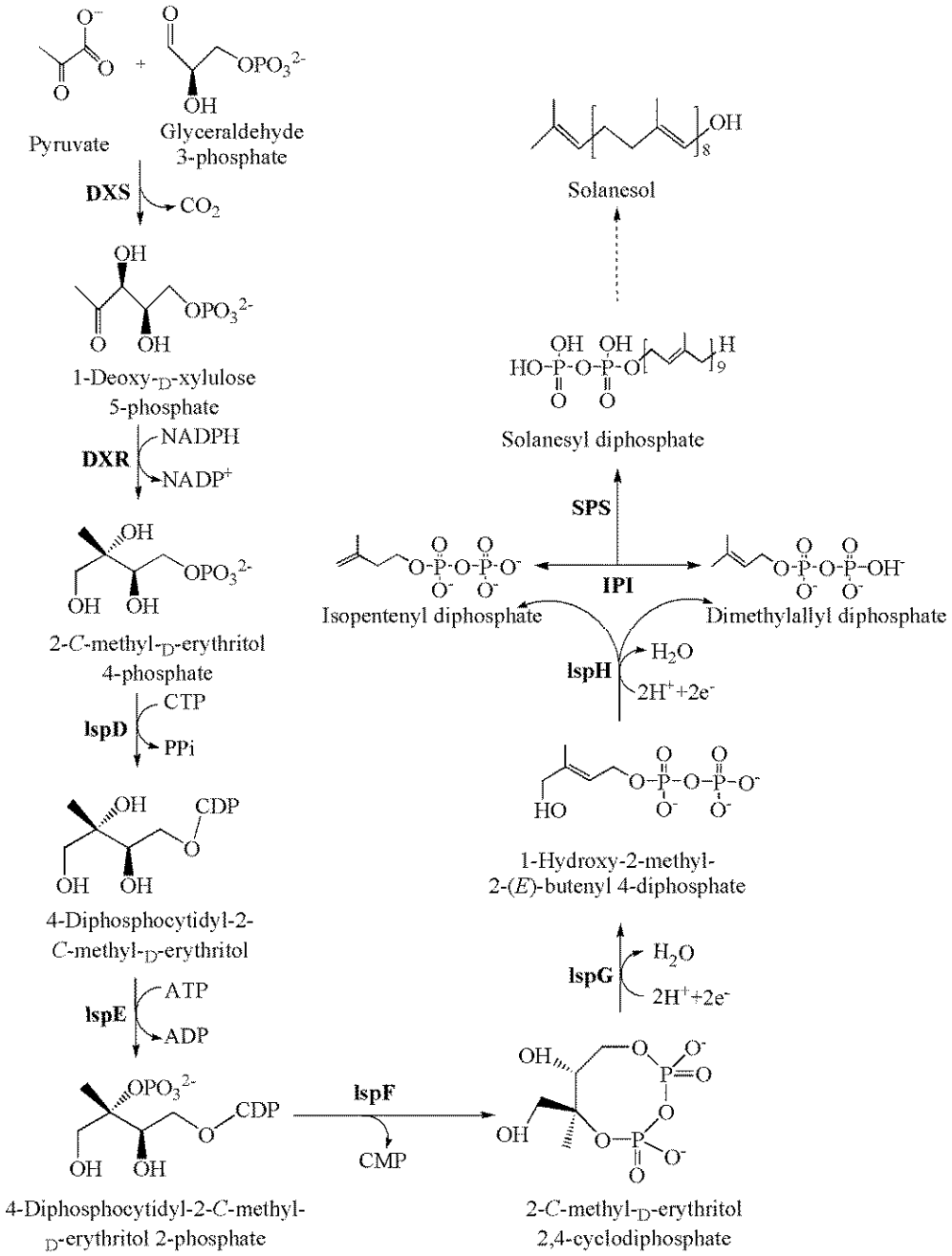

Figure 1. The solanesol biosynthetic pathway in the plastids of tobacco plants. Enzymes in the solanesol biosynthetic pathway are abbreviated as follows: DXS, 1-deoxy-D-xylulose 5-phosphate synthase; DXR, 1-deoxy-D-xylulose 5-phosphate reductoisomerase; IspD, 2-*C*-methyl-D-erythritol 4-phosphate cytidylyltransferase; IspE, 4-diphosphocytidyl-2-*C*-methyl-D-erythritol kinase; IspF, 2-*C*-methyl-D-erythritol 2,4-cyclodiphosphate synthase; IspG, 1-hydroxy-2-methyl-2-(*E*)-butenyl 4-diphosphate synthase; IspH, 1-hydroxy-2-methyl-2-(*E*)-butenyl 4-diphosphate reductase; IPI, isopentenyl diphosphate isomerase; SPS, solanesyl diphosphate synthase.

Therefore, based on significant differences in the solanesol content of tobacco leaves, stems, and roots, the objective of this study was to conduct RNA-seq analysis, to identify transcripts that encoded enzymes involved in solanesol biosynthesis. The study was to characterize two full-length *N. tabacum SPS* cDNA sequences (*NtSPS1* and *NtSPS2*) and to determine their expression patterns and phylogenetic relationships. This work provides important insights into the molecular mechanisms of solanesol biosynthesis in tobacco, as well as in other solanaceous plants, and also contributes to the genetic engineering of tobacco plants with increased solanesol production.

Peer-reviewed version available at *Molecules* **2016**, *21*, 1536; doi:10.3390/molecules21111536

2. Results

2.1. Organ- and growing stage-specific variation in solanesol content

The solanesol content was highest in the leaves of S3-stage tobacco plants, followed by that in the stems and roots ($P < 0.05$) (Figure 2A), and the levels of total solanesol, free-state solanesol, and bound-state solanesol in the leaves were 21.45, 21.23, and 21.70 folds of those in the stems, respectively (Figure 2A). Meanwhile, no measurable solanesol was detected in the roots (Figure 2A). Leaves collected from the four growing stages of plants exhibited significant differences in the content of total solanesol, as well as in that of free- and bound-state solanesol. The content was lowest at the S1 stage, increased at the S2 stage, reached a maximum level at the S3 stage, and then decreased slightly at the S4 stage (Figure 2B).

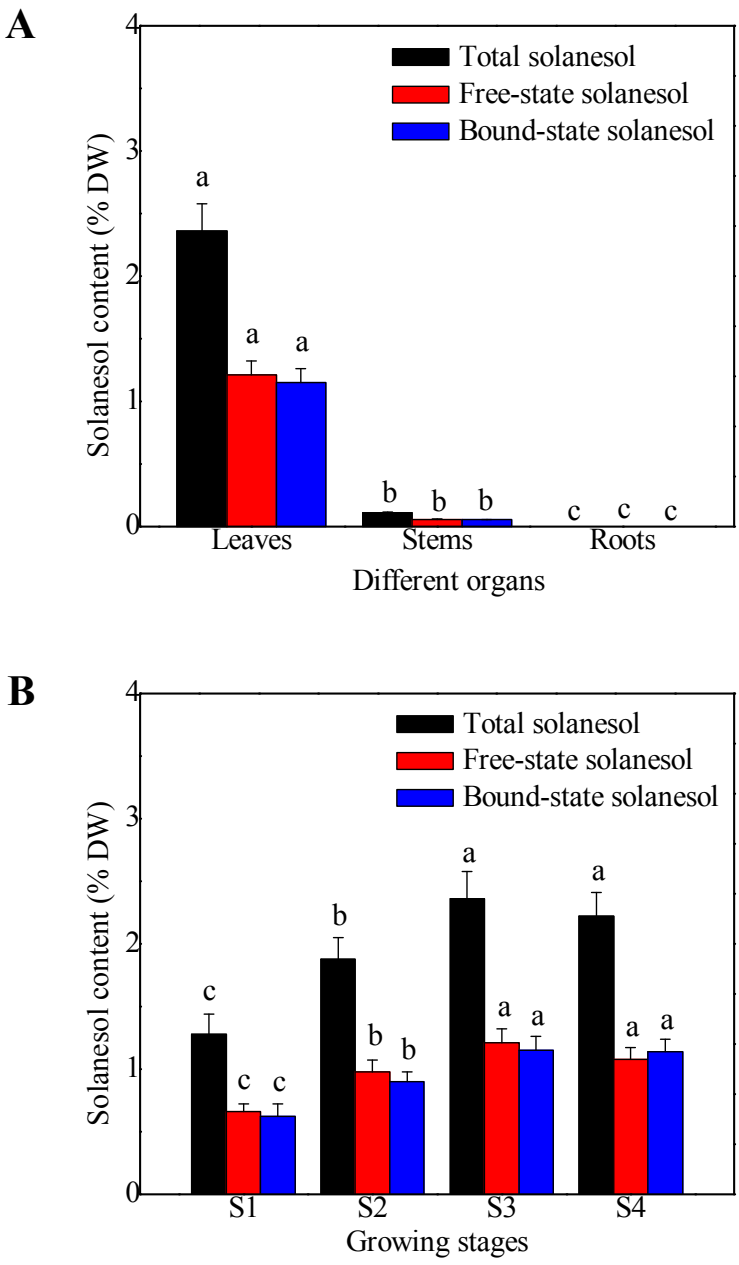

Figure 2. Solanesol content in tobacco plants. (A) Solanesol content in different organs of S3-stage tobacco plants. (B) Solanesol in leaves harvested from four growing stages of tobacco plants. Each value is shown by means ± SD. Different letters on the bars indicate treatments were significantly different at $P < 0.05$. S1, 10 d after transplanting; S2, 20 d after transplanting; S3, 40 d after transplanting; S4, 60 d after transplanting. DW, dry weight.

2.2. Organ-specific expression of solanesol biosynthesis genes

In the present study, six *DXS*, two *DXR*, two *IspD*, four *IspE*, two *IspF*, four *IspG*, two *IspH*, six *IPI*, and two *SPS* genes were identified to be involved in solanesol biosynthesis (Table 1). The FPKM values of *DXS1*, *DXS2*, *DXS5*, and *DXS6* in the three organs decreased in the order: stems > leaves > roots; the values of *DXS4* decreased in the order: stems > roots > leaves; and those of *DXS3* decreased in the order: leaves > stems > roots.

The FPKM values of *DXR1* and *DXR2* in the three organs decreased in the order: leaves > stems > roots, and the FPKM values of *DXR1* and *DXR2* in the leaves were 2.16 and 1.80 folds of those in the stems, respectively, whereas those in the stems were 1.12 and 3.93 folds of those in the roots, respectively (Table 1).

Table 1. Expression of solanesol biosynthesis genes in the leaves, stems, and roots of tobacco plants. The expression levels are expressed as fragments per kilobase of exon per million fragments mapped (FPKM) values.

Gene ID	Function Annotation	Gene abbreviation	Leaves	Stems	Roots
Ntab0104070	1-deoxy-D-xylulose-5-phosphate synthase [*Capsicum annuum*]	*DXS1*	21.9375	62.0806	4.9073
Ntab0137200	1-deoxy-D-xylulose-5-phosphate synthase [*Capsicum annuum*]	*DXS2*	33.9788	43.3916	7.36163
Ntab0429490	1-deoxy-D-xylulose-5-phosphate synthase [*Arabidopsis thaliana*]	*DXS3*	4.15744	3.88924	2.71727
Ntab0604300	1-deoxy-D-xylulose-5-phosphate synthase 2 [*Oryza sativa*]	*DXS4*	0.933736	3.84373	1.18076
Ntab0667680	1-deoxy-D-xylulose-5-phosphate synthase [*Capsicum annuum*]	*DXS5*	5.67963	7.61805	4.11298
Ntab0863750	1-deoxy-D-xylulose-5-phosphate synthase 2 [*Oryza sativa*]	*DXS6*	1.10129	8.57813	0.876698
Ntab0057390	1-deoxy-D-xylulose 5-phosphate reductoisomerase [*Mentha piperita*]	*DXR1*	20.0789	9.30922	8.27978
Ntab0119750	1-deoxy-D-xylulose 5-phosphate reductoisomerase [*Mentha piperita*]	*DXR2*	41.7743	23.1798	5.89792
Ntab0014700	2-C-methyl-D-erythritol 4-phosphate cytidylyltransferase [*Arabidopsis thaliana*]	*IspD1*	10.8564	9.50503	2.87458
Ntab0479870	2-C-methyl-D-erythritol 4-phosphate cytidylyltransferase [*Arabidopsis thaliana*]	*IspD2*	3.66779	5.06216	2.50075
Ntab0204750	4-diphosphocytidyl-2-C-methyl-D-erythritol kinase [*Solanum lycopersicum*]	*IspE1*	7.55806	7.35381	2.79413
Ntab0204760	4-diphosphocytidyl-2-C-methyl-D-erythritol kinase [*Solanum lycopersicum*]	*IspE2*	1.15533	0.553088	0.368872
Ntab0786730	4-diphosphocytidyl-2-C-methyl-D-erythritol kinase [*Solanum lycopersicum*]	*IspE3*	12.1952	8.00878	1.95866
Ntab0826890	4-diphosphocytidyl-2-C-methyl-D-erythritol kinase [*Solanum lycopersicum*]	*IspE4*	12.366	8.07586	3.90324
Ntab0883640	2-C-methyl-D-erythritol 2,4-cyclodiphosphate synthase [*Catharanthus roseus*]	*IspF1*	12.0181	7.88888	3.87722
Ntab0907560	2-C-methyl-D-erythritol 2,4-cyclodiphosphate synthase [*Catharanthus roseus*]	*IspF2*	10.9503	6.10343	2.4778

Ntab0346180	4-hydroxy-3-methylbut-2-en-1-yl diphosphate synthase [*Arabidopsis thaliana*]	*IspG1*	96.1816	41.3238	17.5079
Ntab0578920	4-hydroxy-3-methylbut-2-en-1-yl diphosphate synthase [*Arabidopsis thaliana*]	*IspG2*	37.0178	21.5853	7.08214
Ntab0763840	4-hydroxy-3-methylbut-2-en-1-yl diphosphate synthase [*Arabidopsis thaliana*]	*IspG3*	0.078068	0.090173	0.041577
Ntab0829890	4-hydroxy-3-methylbut-2-en-1-yl diphosphate synthase [*Arabidopsis thaliana*]	*IspG4*	46.6078	24.7031	10.6374
Ntab0167890	4-hydroxy-3-methylbut-2-enyl diphosphate reductase [*Arabidopsis thaliana*]	*IspH1*	143.609	70.7924	21.4238
Ntab0212660	4-hydroxy-3-methylbut-2-enyl diphosphate reductase [*Arabidopsis thaliana*]	*IspH2*	156.544	74.081	15.2902
Ntab0340070	Isopentenyl-diphosphate Delta-isomerase [*Camptotheca acuminata*]	*IPI1*	2.39271	16.7042	24.35
Ntab0353610	Isopentenyl-diphosphate Delta-isomerase [*Camptotheca acuminata*]	*IPI2*	5.23626	14.1152	43.6775
Ntab0520040	Isopentenyl-diphosphate Delta-isomerase [*Camptotheca acuminata*]	*IPI3*	42.5927	80.1313	57.5339
Ntab0881480	Isopentenyl-diphosphate Delta-isomerase [*Arabidopsis thaliana*]	*IPI4*	43.1744	41.642	46.4998
Ntab0901260	Isopentenyl-diphosphate Delta-isomerase [*Camptotheca acuminata*]	*IPI5*	40.7304	20.0821	58.6209
Ntab0958550	Isopentenyl-diphosphate Delta-isomerase [*Camptotheca acuminata*]	*IPI6*	2.36834	16.3683	18.7175
Ntab0214390	Solanesyl diphosphate synthase 1 [*Arabidopsis thaliana*]	*SPS1*	89.5248	6.91123	0.89861
Ntab0720120	Solanesyl diphosphate synthase 1 [*Arabidopsis thaliana*]	*SPS2*	80.73	8.42459	1.63294

The FPKM values of *IspD1* in the three organs decreased in the order: leaves > stems > roots, and those of *IspD2* decreased in the order: stems > leaves > roots (Table 1). The FPKM value of *IspD1* in the leaves was 1.14 fold of that in the stems, and the FPKM value of *IspD2* in the stems was 1.38 fold of that in the leaves. The FPKM values of *IspD1* and *IspD2* in the stems were 3.31 and 2.02 folds of those in the roots, respectively.

The FPKM values of *IspE1*, *IspE2*, *IspE3*, and *IspE4* in the three tobacco organs decreased in the order: leaves > stems > roots (Table 1). The FPKM values of *IspE1*, *IspE2*, *IspE3*, and *IspE4* in the leaves were 1.02, 2.09, 1.52, and 1.53 folds of those in the stems, respectively, and those in the stems were 2.63, 1.50, 4.09, and 2.07 folds of those in the roots, respectively.

The FPKM values of *IspF1* and *IspF2* in the three organs decreased in the order: leaves > stems > roots (Table 1). The FPKM values of *IspF1* and *IspF2* in the leaves were 1.52 and 1.79 folds of those in the stems, and those in the stems were 1.03 and 2.46 folds of those in the roots, respectively.

The FPKM values of *IspG1*, *IspG2*, and *IspG4* in the three organs decreased in the order: leaves > stems > roots, and those of *IspG3* followed the order: stems > leaves > root (Table 1). The FPKM values of *IspG1*, *IspG2*, *IspG3*, and *IspG4* in the leaves were 2.33, 1.71, 0.87, and 1.89 folds of those in the stems, respectively, and those in the stems were 2.36, 3.05, 2.17, and 2.32 folds of those in the roots, respectively.

The FPKM values of *IspH1* and *IspH2* in the three organs decreased in the order: leaves > stems > roots (Table 1). The FPKM values of *IspH1* and *IspH2* in the leaves were 2.03 and 2.11 folds of those in the stems, whereas those in the stems were 3.30 and 4.84 folds of those in the roots, respectively.

The FPKM values of *IPI1*, *IPI2*, and *IPI6* in the three organs decreased in the order: roots > stems > leaves, whereas those of *IPI3* followed the order: stems > roots > leaves, and those of *IPI4* and *IPI5* followed the order: roots > leaves > stems (Table 1). The FPKM values of *IPI1*, *IPI2*, and *IPI6* in the

roots were 1.46, 3.09, and 1.14 folds of those in the stems, respectively, whereas those in the stems were 6.98, 2.70, and 6.91 folds of those in the leaves, respectively.

The FPKM values of *SPS1* and *SPS2* in the three organs decreased in the order: leaves > stems > roots (Table 1). The FPKM values for *SPS1* and *SPS2* in the leaves were 12.95 and 9.58 folds of those in the stems, respectively, whereas those in the stems were 7.69 and 5.16 folds of those in the roots, respectively.

2.3. Organ- and growing stage-specific NtSPS expression

The relative expression of *NtSPS* genes was significantly higher in the leaves of the tobacco plants than in the stems and roots ($P < 0.05$), in which the *NtSPS* levels were statistically similar ($P > 0.05$) (Figure 3A), and the relative expression of *NtSPS1* and *NtSPS2* in the leaves was 13.19 and 10.17 folds of those in the stems, respectively. In addition, the relative expression of *NtSPS1* and *NtSPS2* also differed significantly among the leaves from the four growing stages. The expression was lowest at the S1 stage, increased at the S2 stage, peaked at the S3 stage, and the decreased at the S4 stage (Figure 3B). Therefore, the relative expression of *NtSPS1* and *NtSPS2* was consistent with the content of solanesol measured in the four growing stages.

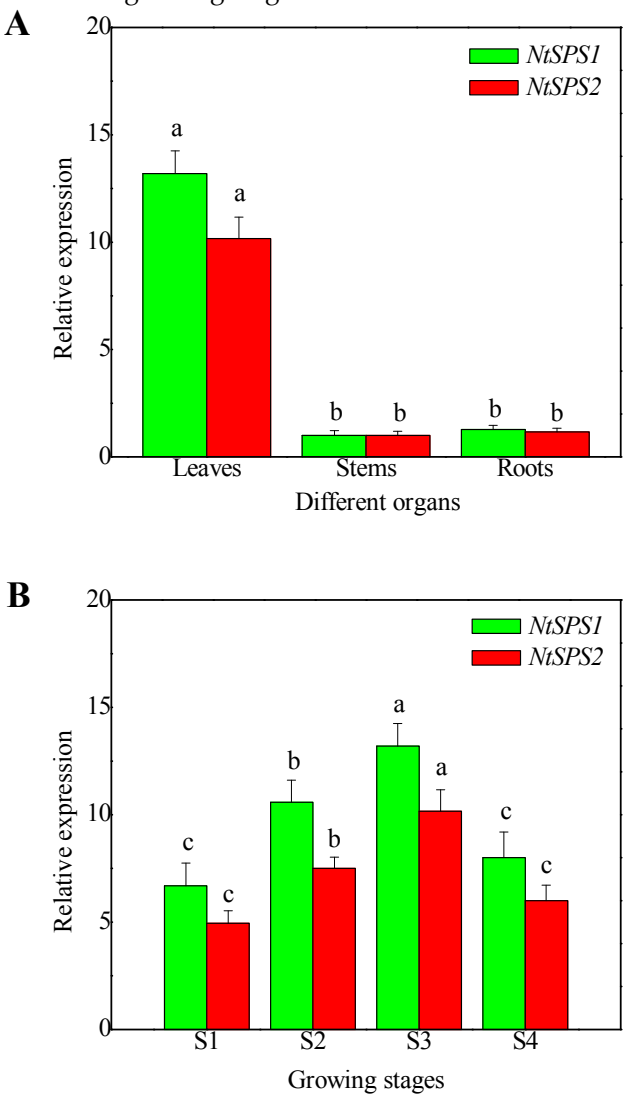

Figure 3. Relative expression of solanesyl diphosphate synthase (*NtSPS*) in tobacco plants. (A) *NtSPS* expression in different organs of S3-stage tobacco plants. (B) *NtSPS* expression in leaves harvested from four growing stages of tobacco plants. Each value is shown by means ± SD. Different letters on the bars indicate treatments were significantly different at $P < 0.05$. S1, 10 d after transplanting; S2, 20 d after transplanting; S3, 40 d after transplanting; S4, 60 d after transplanting.

2.4. Phylogenetic analysis of NtSPS

In the phylogenetic analysis of the 37 SPS sequences, the SPS genes of tobacco (*NtSPS1* and *NtSPS2*) clustered with those from other solanaceous plants, such as *Solanum lycopersicum*, *S. pennellii*, and *S. tuberosum* (Figure 4), and the SPS genes from brassicaceous plants (e.g., *Arabidopsis thaliana*, *B. napus*, *B. oleracea* var. oleracea, and *B. rapa*) also formed a distinct cluster. In addition, multiple sequence alignment of the SPS amino acid sequences from *A. thaliana*, *B. napus*, tomato, and tobacco revealed the presence of two conserved aspartate-rich DDxxD domains (Figure 5).

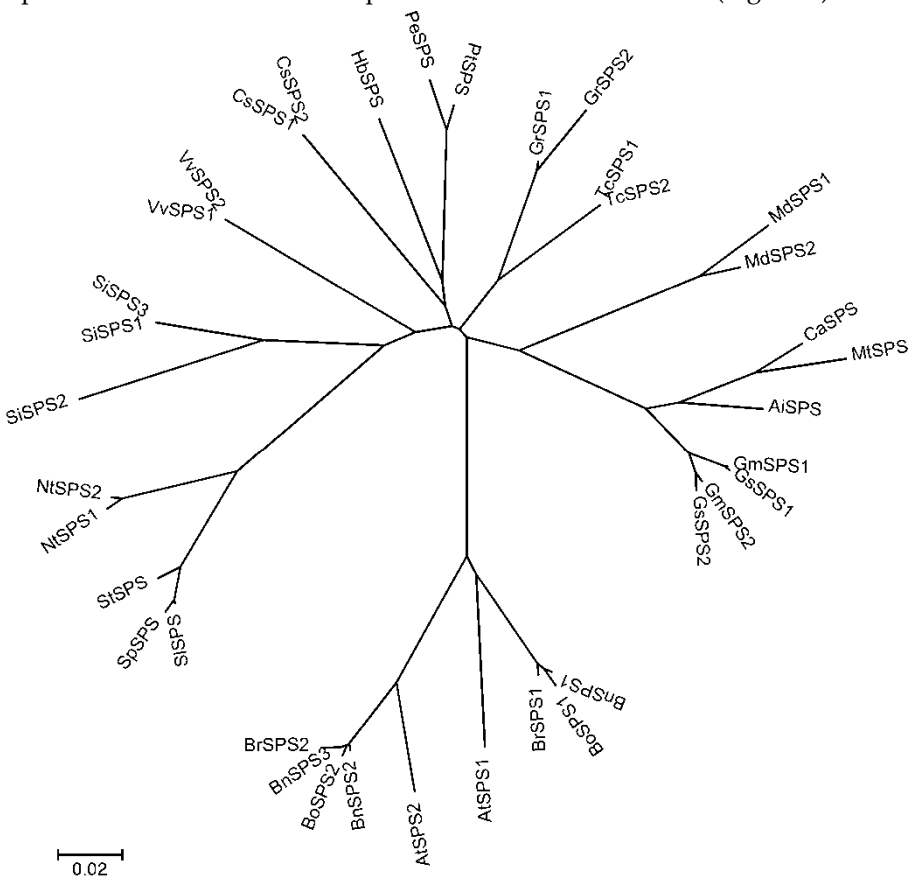

Figure 4. Molecular phylogenetic tree constructed using the amino acid sequences of solanesyl diphosphate synthase (SPS) from different plants. The tree was constructed using the neighbour-joining method in MEGA 5.0. Enzymes used for alignment are as follows: AiSPS (*Arachis ipaensis*, XP_016171459.1), AtSPS1 (*Arabidopsis thaliana*, ABF58968.1), AtSPS2 (*Arabidopsis thaliana*, NP_173148.2), BnSPS1 (*Brassica napus*, XP_013649976.1), BnSPS2 (*Brassica napus*, XP_013660438.1), BnSPS3 (*Brassica napus*, XP_013641601.1), BoSPS1 (*Brassica oleracea* var. oleracea, XP_013592833.1), BoSPS2 (*Brassica oleracea* var. oleracea, XP_013637933.1), BrSPS1 (*Brassica rapa*, XP_009106560.1), BrSPS2 (*Brassica rapa*, XP_009149144.1), CaSPS (*Cicer arietinum*, XP_004488673.1), CsSPS1 (*Citrus sinensis*, XP_015385554.1), CsSPS2 (*Citrus sinensis*, XP_015385553.1), GmSPS1 (*Glycine max*, XP_003543173.1), GmSPS2 (*Glycine max*, XP_003546746.1), GrSPS1 (*Gossypium raimondii*, XP_012462942.1), GrSPS2 (*Gossypium raimondii*, XP_012462943.1), GsSPS1 (*Glycine soja*, KHN47455.1), GsSPS2 (*Glycine soja*, KHN39753.1), HbSPS (*Hevea brasiliensis*, ABD92707.1), MdSPS1 (*Malus domestica*, XP_008363649.1), MdSPS2 (*Malus domestica*, XP_008386386.1), MtSPS (*Medicago truncatula*, XP_013464447.1), PeSPS (*Populus euphratica*, XP_011045575.1), PtSPS (*Populus trichocarpa*, XP_002300442.2), SiSPS1 (*Sesamum indicum*, XP_011098150.1), SiSPS2 (*Sesamum indicum*, XP_011082816.1), SiSPS3 (*Sesamum indicum*, XP_011098151.1), SlSPS (*Solanum lycopersicum*, XP_004244308.1), SpSPS (*Solanum pennellii*, XP_015082582.1), StSPS (*Solanum tuberosum*, XP_006348350.1), TcSPS1 (*Theobroma cacao*, XP_007022091.1), TcSPS2 (*Theobroma cacao*, XP_007022090.1), VvSPS1 (*Vitis vinifera*, XP_002285665.1), and VvSPS2 (*Vitis vinifera*, XP_010644050.1).

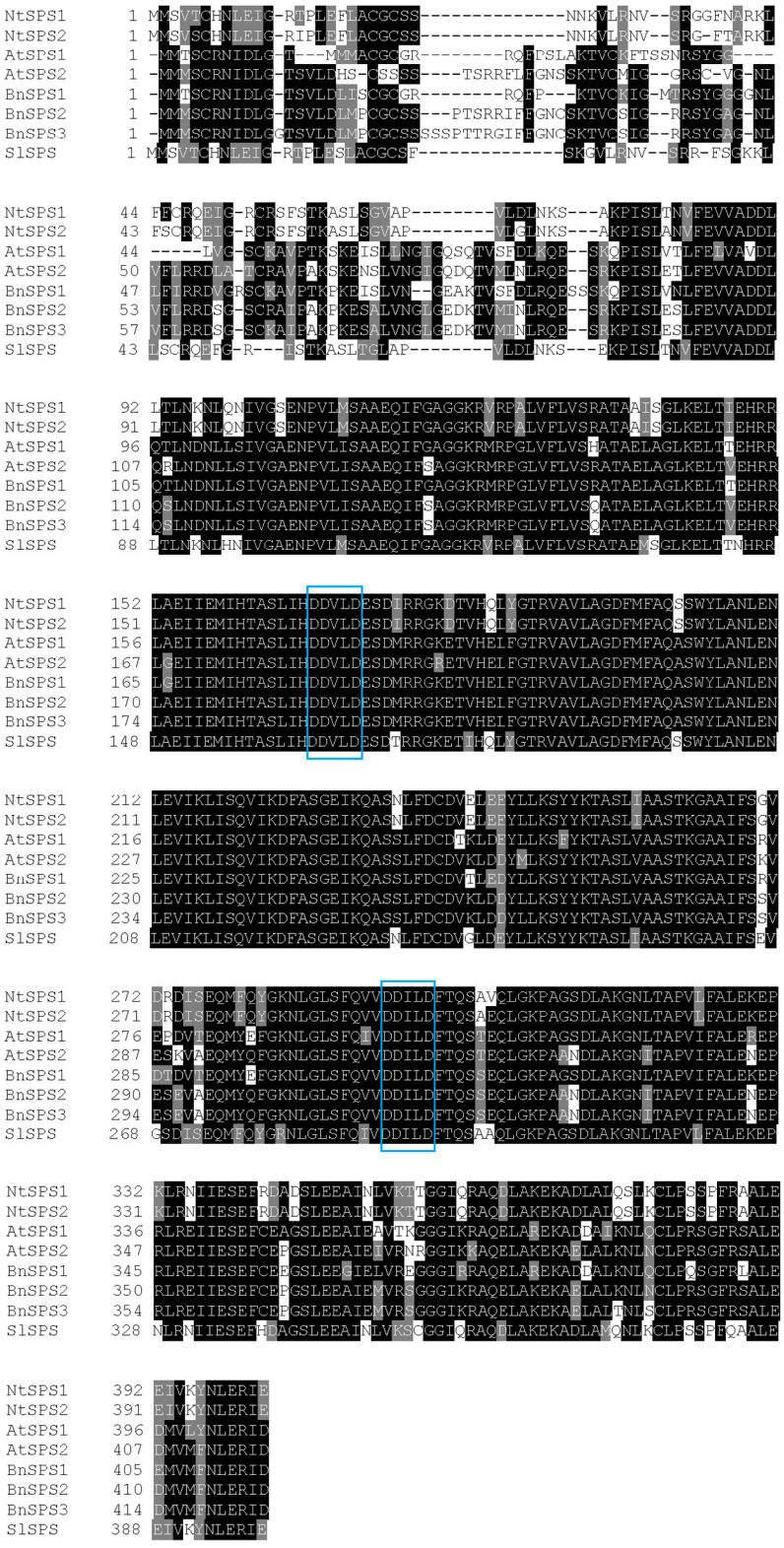

Figure 5. Multiple sequence alignment of solanesyl diphosphate synthase (SPS) from tobacco (*Nicotiana tabacum*), tomato (*Lycopersicon esculentum*), *Arabidopsis thaliana*, and *Brassica napus*. The conserved functional motif, DDxxD, is boxed in blue. Identical and similar amino acid residues are shaded in black and grey respectively. The alignment of the full-length predicted amino acid sequences was performed using MultiAlign and shaded using BOXSHADE 3.21 (http://www.ch.embnet.org/software/BOX_form.html). AtSPS1 (*Arabidopsis thaliana*, ABF58968.1), AtSPS2 (*Arabidopsis thaliana*, NP_173148.2), BnSPS1 (*Brassica napus*, XP_013649976.1), BnSPS2 (*Brassica napus*, XP_013660438.1), BnSPS3 (*Brassica napus*, XP_013641601.1), and SlSPS (*Solanum lycopersicum*, XP_004244308.1)

2.5. Organ- and growing stage-specific chlorophyll content

The total chlorophyll, chlorophyll a, and chlorophyll b content were highest in leaves of the S3-stage tobacco plants, followed by the levels detected in the stems and roots, respectively ($P < 0.05$) (Figure 6A). In the leaves, the content of total chlorophyll, chlorophyll a, and chlorophyll b were 23.05, 28.33, and 14.78 folds of those in the stems, respectively (Figure 6A), and no chlorophyll was detected in the roots. Significant differences in chlorophyll content were also observed in the leaves collected from four growing stages, and all three levels were lowest at the S1 stage, increased at the S2 stage, peaked at the S3 stage, and decreased at the S4 stage (Figure 6B). These changes were consistent with the distribution of solanesol in the three organs and the levels of solanesol detected at four growing stages.

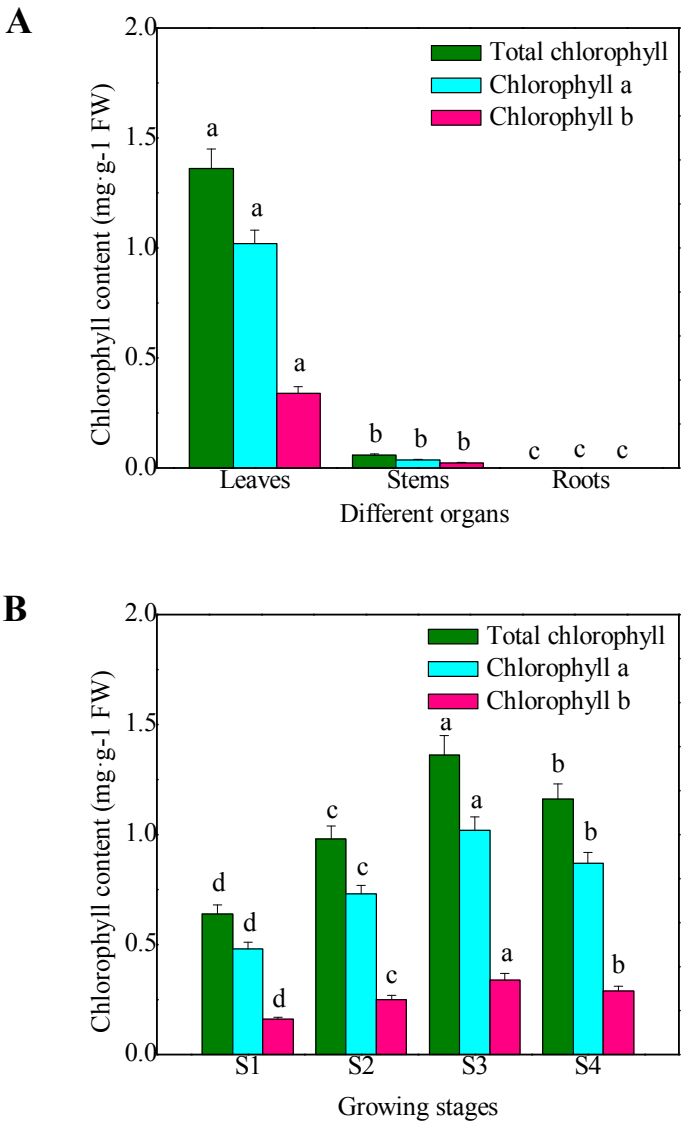

Figure 6. Chlorophyll content in tobacco plants. (A) Chlorophyll content in different organs of S3-stage tobacco plants. (B) Chlorophyll content in leaves harvested from four growing stages of tobacco plants. Each value is shown by means ± SD. Different letters on the bars indicate treatments were significantly different at $P < 0.05$. S1, 10 d after transplanting; S2, 20 d after transplanting; S3, 40 d after transplanting; S4, 60 d after transplanting. FW, fresh weight.

3. Discussion

3.1. Solanesol is abundant in tobacco leaves

Solanesol is a long-chain polyisoprenoid alcohol that mainly accumulates in solanaceous plants, especially tobacco [1,3,12], and is an important intermediate in the synthesis of ubiquinones and anti-cancer drugs. Because the chemical synthesis of solanesol is difficult [11], we assessed some aspects of its biosynthesis in tobacco plants and observed differential accumulation of solanesol in the leaves, stems, and roots of tobacco plants, with the content in leaves being the highest (Figure 2A). Thus, tobacco leaves could be the ideal material for extracting solanesol [3,12]. The results revealed that the solanesol content of leaves varied with growing stage and was highest in leaves from plants in the S3 stage (40 d after transplanting; Figure 2B). Therefore, the S3 stage can be considered as the most appropriate period for harvesting tobacco leaves for solanesol extraction. However, since the accumulation of solanesol is reportedly influenced by genetic and environmental factors [1,3,12,15], for the optimal extraction of solanesol from fresh tobacco leaves, the appropriate harvesting period was suggested to be determined for individual tobacco varieties and their specific environmental conditions.

3.2. Solanesol biosynthesis genes were identified in tobacco plants

Based on the names of key enzymes in solanesol biosynthesis, as summarized by Yan et al. [3], the present study demonstrated that six *DXS*, two *DXR*, two *IspD*, four *IspE*, two *IspF*, four *IspG*, two *IspH*, six *IPI*, and two *SPS* genes were involved in the biosynthesis of solanesol in tobacco (Table 1), and previous studies have shown that solanesol biosynthesis occurs in the plastids of tobacco plants *via* the MEP pathway [3,12,14].

DXS is the first enzyme in the MEP pathway, where it catalyses the conversion of pyruvate and glyceraldehyde 3-phosphate to form 1-deoxy-D-xylulose 5-phosphate (DXP) (Figure 1) [3,12]. In *Medicago truncatula*, *MtDXS1* was preferentially expressed in several above-ground tissues (e.g., leaves, stem) but not in in the roots (Table 1), whereas *MtDXS2* transcript levels were low in most tissues but were strongly stimulated in roots upon colonization by mycorrhizal fungi [16]. Compared with non-transgenic wild-type plants, transgenic *Arabidopsis* plants that overexpressed or underexpressed the *DXS* gene accumulated different levels of various isoprenoids, including chlorophylls, tocopherols, carotenoids, abscisic acid, and gibberellins [17], and when the *A. thaliana DXS* gene was constitutively expressed in spike lavender, the transgenic plants accumulated significantly more essential oils (monoterpenes) in their leaves and flowers [18]. Thus, as an important regulatory factor in the MEP pathway, DXS is the first enzyme involved in solanesol biosynthesis, and the overexpression or inhibition of its expression can lead to changes in the content of downstream metabolites.

Meanwhile, DXR catalyses the intramolecular rearrangement of DXP's straight-chain carbon skeleton to MEP (Figure 1) [3,12]. In the present study, the variation in FPKM values of *DXR1* and *DXR2* in leaves, stems, and roots (Table 1) was consistent with the distribution of solanesol (Figure 2). Zhang et al. [19] cloned two *DXR* genes from *N. tabacum*, and found that the expression levels of *NtDXR1* and *NtDXR2* were highest in tobacco leaves, followed by those in the stem and roots. The down-regulation of *DXR* in *A. thaliana* results in variegation, reduced pigmentation, and defects in chloroplast development, whereas *DXR*-overexpressing lines exhibit increased accumulation of MEP-derived plastid isoprenoids, such as chlorophylls and carotenoids [20]. Overexpression of the tobacco *DXR* gene in chloroplasts was also shown to contribute to increased isoprenoid production, including solanesol, chlorophyll a, beta-carotene, lutein, antheraxanthin, and beta-sitosterol [21]. Therefore, DXR is obviously another key enzyme in the biosynthesis of solanesol in tobacco, and its overexpression in chloroplasts can promote the accumulation of solanesol.

IspD, IspE, IspF, IspG, and IspH sequentially catalyse the transformation of MEP to IPP and DMAPP (Figure 1) [3,22]. In the present study, we found that the FPKM values of the different *Isp* genes in the three organs varied (Table 1), and the relative expression of *IspE*, *IspF*, *IspG*, and *IspH* was higher in the tobacco leaves and stems than in the roots. Similarly, Hsieh et al. [23] observed that

IspD1, *IspD2*, and *IspE1* were mainly expressed in the leaves and stems of *A. thaliana*. However, Kim et al. [24] cloned an *IspF* gene from *Ginkgo biloba* and found that its expression was higher in embryonic roots than in embryonic leaves. Gao et al. [25] also reported that the expression of *IspF* was highest in *G. biloba* roots, followed by that in the leaves and seeds, respectively, and Lu et al. [26] cloned the *IspH* gene from *G. biloba* and found that its expression was also highest in roots, followed by its expression in stems and leaves. Kim et al. [27] cloned two *IspH* genes from *G. biloba* and found that the expression of *IspH1* was higher in the leaves than in the roots, whereas the expression of *IspH2* was higher in the roots than in the leaves. Thus, our results regarding the distribution of *IspD*, *IspE*, *IspF*, *IspG*, and *IspH* expression are not fully consistent with those of previous studies in other plants.

IPI catalyses the isomerization of IPP and DMAPP and requires Mg^{2+} for its activity, and DMAPP can then bind to IPP to form isoprenoids, such as solanesol (Figure 1) [3,28]. In the present study, we assessed the FPKM values of different *IPI* genes in the leaves, stems, and roots of tobacco plants (Table 1). Nakamura et al. [29] cloned two *N. tabacum IPI* genes and found that the expression of *IPI1* increased under high-salt and high-light stress conditions, whereas the expression of *IPI2* increased under high-salt and cold stress conditions. Sun et al. [30] cloned an *IPI* gene from *S. lycopersicum* and found that its expression was highest in roots, followed by that in stems and leaves, which was consistent with the distribution of *IPI1*, *IPI2*, and *IPI6* expression observed in the present study.

3.3. SPS is a key enzyme in solanesol biosynthesis in tobacco

SPS catalyses the reaction of IPP and DMAPP to form SPP, which is a precursor of solanesol and plastoquinone (Figure 1) [3,12]. In the present study, both qRT-PCR and RNA-seq analyses indicated that the relative expression levels of *NtSPS1* and *NtSPS2* were significantly higher in leaves than in stems and roots ($P < 0.05$). To date, *SPS* homologs have been identified in *A. thaliana* [31–33], *Hevea brasiliensis* [34], *Oryza sativa* [35], and *S. lycopersicum* [36]. Hirooka et al. [32] cloned two *SPS* genes from *A. thaliana* and found that the expression levels of *AtSPS1* and *AtSPS2* in leaves and stems were significantly higher than those in the roots, which is similar to the expression of *NtSPS1* and *NtSPS2* observed in the present study (Figure 3). Phatthiya et al. [34] also cloned an *SPS* gene from *H. brasiliensis* and found its expression was higher in leaves and stems than in roots, and Ohara et al. [35] cloned two *SPS* genes from *O. sativa* and reported that *OsSPS1* was highly expressed in root tissue, whereas *OsSPS2* was highly expressed in both leaves and roots. Thus, the distribution of *SPS* expression may be species specific.

The homology among NtSPS1, NtSPS2, and SPS in other solanaceous plants was observed to be relatively higher than that in other families (Figure 4), and our results suggest that the biological function of SPSs in solanaceous plants is similar to that reported in other plants [37]. SPSs from other plants contain two conserved aspartate-rich DDxxD domains (Figure 5), which are involved in the coordination of divalent metal ions with the diphosphate groups in substrates and play a key role in substrate positioning [38]. Jones et al. [36] suggested that the constitutive overexpression of *SlSPS* in tobacco could significantly increase the plastoquinone content in immature leaves, as well as the solanesol content in the mature leaves, and also reported that the solanesol content in the mature leaves of transgenic tobacco plants was positively correlated with the expression of *SlSPS*. Thus, SPS is a key enzyme in the solanesol biosynthetic pathway, and its overexpression can promote the accumulation of downstream metabolites, such as solanesol [3,12,36].

Our results also revealed that the chlorophyll content in the leaves, stems, and roots of tobacco plants (Figure 6A) was consistent with the distribution of solanesol in these organs (Figure 2A). Moreover, leaves from the four growing stages exhibited significant changes in their chlorophyll content (Figure 6B), which was consistent with the distribution of solanesol in the four stages (Figure 2B). Solanesol biosynthesis occurs in the chloroplast and that SPS is a key enzyme in the solanesol biosynthetic pathway [3,12,14,36]. In the present study, the chlorophyll content, expression of *NtSPS1* and *NtSPS2*, and solanesol content of leaves were significantly higher than those of stems and roots (Figure 2A, Figure 3A, Figure 6A), which further suggests that NtSPS1 and NtSPS2 are key enzymes in solanesol biosynthesis in tobacco.

4. Experimental Section

4.1. Plant materials and growing conditions

N. tabacum (Honghua Dajinyuan) plants were used for RNA-seq analysis. The seed was obtained from China Tobacco Germplasm Platform. The seedlings, which sprouted on February 10, 2014, were transplanted on April 20, 2014. The plants were grown and maintained in plastic containers in a greenhouse at the Tobacco Research Institute of Chinese Academy of Agricultural Sciences (Qingdao, China) under natural conditions (16 h light at 28 °C during the day, 8 h dark at 23 °C during the night). The plants were maintained in soil (pH: 7.2, total N: 1.89 g/kg, alkali-soluble N: 48.3 mg/kg, total P 0.45 g/kg, available P: 32.4 mg/kg, total K: 32.5 g/kg, available K: 219 mg/kg, organic matter: 7.39 g/kg). Then, to determine solanesol and chlorophyll content and to perform RNA-seq and quantitative real-time PCR (qRT-PCR) analyses, the leaf tissues were harvested from four growing stages of tobacco plants, e.g. sample S1, S2, S3, and S4 were harvested at 10, 20, 40, and 60 d after transplanting, respectively, and root, stem, and leaf samples were harvested from S3-stage plants. All the experiments were performed in triplicate.

4.2. Analysis of total, free-state, and bound-state solanesol content

Tobacco leaves, stems, and roots were dried to constant weight with a freeze-dryer (Alpha 1-2 LD Plus; Christ, Osterode am Harz, Germany), ground, and sifted through a 40-mesh sieve. The powdered samples (2 g) were placed in individual 50-mL centrifuge tubes with stoppers and 20 mL hexane was added. Ultrasonic extraction was performed at 65 °C for 15 min, followed by 10-min centrifugation of the homogenates. The supernatants were transferred to 50-mL volumetric flasks, and then the extraction steps were repeated by extracting the precipitated layers two more times, with 15 mL hexane, both of which were combined with the initial 20 mL extractant from each sample.

To prepare the samples for quantification of free-state solanesol, 4 mL of each hexane extract was transferred to individual 10-mL stoppered centrifuge tubes and supplemented with 6 mL distilled water. The mixtures were vortexed for 3 min to remove the water-soluble impurities and then centrifuged for 10 min. Next, the upper layers were removed, diluted with a methanol-acetonitrile (50:50, v:v) solution in brown volumetric flasks, and then filtered through a 0.2-μm membrane, prior to analysis.

Meanwhile, to prepare the samples for quantification of total solanesol, 4 mL of each of the extracts was transferred to individual 100-mL brown stoppered flasks and supplemented with 4 mL 0.02 M NaOH (diluted in ethanol). After thorough mixing, the mixtures were oscillated in a water bath for 30 min at 60–65 °C to allow saponification and then incubated in an 83–87 °C water bath to allow the solvent to evaporate. Subsequently, hexane (2 mL) was added and the samples were subject to ultrasonication for 2 min, in order to dissolve the residue. The mixture was transferred to a clean 10-mL stoppered centrifuge tube, and another 2 mL hexane was added to dissolve the residue. Thereafter, 6 mL distilled water was added, and the mixtures were vortexed for 3 min to remove the water-soluble impurities. After a 10-min centrifugation, the upper layers were removed, diluted with a methanol-acetonitrile (50:50, v:v) solution in brown volumetric flasks, and then filtered through a 0.2-μm membrane, prior to the estimation.

The amounts of total and free-state solanesol were measured using ultra-high performance liquid chromatography (ACQUITY UPLC H-Class; Waters, Milford, MA, USA) with an Atlantis T3-C_{18} column (4.6×150 mm, 3 μm; Waters) that was maintained at 35 °C. A methanol-acetonitrile (50:50, v:v) solution was used as the mobile phase at a flow rate of 1.0 mL/min, and a diode array detector was used for detection at 213 nm. Finally, the amount of bound-state solanesol in each extract was calculated as the difference between the free-state and total solanesol levels.

4.3. Preparation of digital gene expression library, sequencing, and analysis

The roots, stems, and leaves collected from S3-stage tobacco plants were used to generate three digital gene expression libraries, in order to identify the genes involved in solanesol biosynthesis in

Peer-reviewed version available at *Molecules* **2016**, *21*, 1536; doi:10.3390/molecules21111536

tobacco plants. Plants with possible microbial contamination were excluded. Total RNA was extracted using TRIzol® (Invitrogen, Carlsbad, CA, USA). RNA degradation and contamination was assessed using electrophoresis on 1 % agarose gels. The purity of the extracted RNA was checked spectrophotometrically, using a NanoPhotometer® (Implen, Inc., Westlake Village, CA, USA), and the RNA was quantified using the Qubit® RNA Assay Kit and a Qubit® 2.0 fluorometer (Life Technologies, Carlsbad, CA, USA). The integrity of the RNA was assessed using an RNA Nano 6000 Assay Kit and the BioAnalyzer 2100 system (Agilent Technologies, Santa Clara, CA, USA). Three mixtures containing equal amounts of RNA from the three organs were prepared for each sample and subsequently used to construct the library. The experiments were performed in triplicate, and the libraries were subject to RNA-seq analysis using an Illumina HiSeq™ 2000 platform at the Beijing Genomics Institute (Shenzhen, Guangdong, China).

Since dirty raw reads (i.e., reads with adapters, unknown nucleotides, or quality values ≤5 that accounted for >50 % of the read) would negatively affect downstream analyses, they were discarded. *De novo* assembly of the short reads was performed using the Trinity assembly program, according to the method of Grabherr et al. [39]. Functions of the unigenes were annotated using BLAST, with E-values < 10^{-5}, against protein databases, including the National Center for Biotechnology Information (NCBI) non-redundant (Nr) database (http://www.ncbi.nlm.nih.gov), Universal Protein Resource (UniProt) database (http://www.uniprot.org), and Cluster of Orthologous Groups of proteins (COG) database (http://www.ncbi.nlm.nih.gov/COG). The raw data of the three transcriptomes were used to establish an in-house transcriptome reference database, which was submitted to the China Tobacco Genome (CTG) database (http://218.28.140.17/). For gene expression analysis, the number of expressed sequence tags was calculated and then normalized to fragments per kilobase of exon per million fragments mapped (FPKM) reads, according to the method of Mortazavi et al. [40]. The FPKM values of genes involved in the biosynthesis of solanesol in the three selected tobacco organs were then obtained by searching the full names of the genes in the CTG database (for example, solanesyl diphosphate synthase was used for SPS).

4.4. Screening and cloning of NtSPS

Based on the annotation of unigenes and the FPKM values of the three digital gene expression databases, we identified unigenes associated with solanesol biosynthesis, and the coding sequences of *NtSPS1* and *NtSPS2* were obtained by searching for "solanesyl diphosphate synthase" in the CTG database.

In order to clone the two *NtSPS* genes, total RNA was isolated from tobacco leaves, and its quality was assessed as described in the previous section. In order to obtain first strand cDNA, reverse transcription was performed using a PrimerScript™ RT-PCR kit (Takara Bio, Inc., Shiga, Japan), and the cDNA was used as a template for PCR amplification, using gene-specific primers to amplify the complete coding sequences of both *NtSPS1* (upstream primer: 5′-ATGATGTCTGTGACTTGCCATAATC-3′, downstream primer: 5′-CTATTCAATTCTCTCCAGATTATACTTCAC-3′) and *NtSPS2* (upstream primer: 5′-ATGATGTCTGTGAGTTGCCATAATC-3′, downstream primer 5′-CTATTCAATTCTCTCCAGATTATACTTCAC-3′). The PCR amplification was performed as described by Block et al. [31], and the amplified products were gel extracted and transformed into competent *Escherichia coli* DH5α cells. Finally, the positive clones were screened and sequenced at the Beijing Genomics Institute.

4.5. RNA extraction, cDNA synthesis, and qRT-PCR analysis

Total RNA was extracted from the roots, stems, and leaves of S3-stage tobacco plants, as well as from the leaves of S1-, S2-, and S4-stage plants, as described above. Two micrograms of total extracted RNA from each sample was reverse transcribed to generate first-strand cDNA using the PrimerScript™ kit (Takara Bio, Inc.), according to the manufacturer's instructions, and the experiments were performed in triplicate. Gene-specific primer pairs were designed, using the Primerquest software (http://www.idtdna.com/pages/scitools), for sequence analysis of *NtSPS1*

(upstream primer: 5′-TGTCTGTGACTTGCCATAA-3′, downstream primer 5′-CATTGAATCCTCCTCTACTT-3′) and *NtSPS2* (upstream primer: 5′-CAGTGTTGGGTTTGAATA-3′, downstream primer: 5′-CTTGTTTAGAGTAAGGAGGTC-3′). The qRT-PCR was performed using an ABI 7500 Real-time system (Applied Biosystems, Foster City, CA, USA) with SYBR Premix Ex Taq™ Kit (TaKaRa Bio), according to the manufacturer's protocol and with the following amplification conditions: 95 °C for 2 min, followed by 40 cycles of 95 °C for 15 s and 60 °C for 1 min, and plate reading after each cycle. Two fragments of a constitutively expressed *Ntactin* gene were amplified as a reference, using the gene-specific upstream and downstream primers 5′-CATTCCAAATATGAGATGCGTTGT-3′ and 5′-TGTGGACTTGGGAGAGGACT-3′, respectively.

4.6. Phylogenetic analysis of NtSPS

We aligned SPS amino acid sequences from different plant species using CLUSTAL W, computed the evolutionary distances between the sequences using the Poisson correction method, and constructed a neighbour-joining (NJ) tree using MEGA 5.0 [37]. The reliability of the topology was assessed using the bootstrap re-sampling method with 1000 bootstrap replications. For each analysis, only the nodes supported by bootstrap values >50 % are shown.

4.7. Determination of chlorophyll content

Chlorophyll was extracted from the leaf, stem, and root samples by grinding 0.5 g of each sample in a mortar with 1 mL of 100 % acetone and a pinch of calcium carbonate. The individual extracts were poured into test tubes, after which the mortars were rinsed with 100 % acetone, the rinsates were added to the extracts, and each sample extract was diluted to 5 mL with acetone. Afterward, each of the extracts was filtered through a 0.45-μm syringe filter to remove the debris, and the absorbance of the filtered extract was determined using a UV-2410PC spectrophotometer (Shimadzu, Tokyo, Japan) at 663 nm (A_{663}) and 645 nm (A_{645}). Then the chlorophyll a and chlorophyll b content was calculated using the following equations: C_A = 0.25*(12.7*[A_{663}] - 2.69*[A_{645}]) and C_B = 0.25(22.9[A_{645}] - 4.68*[A_{663}]), where, C_A and C_B are the contents (mg/g) of chlorophyll a and b, respectively [41]. Total chlorophyll content was calculated as the sum of the chlorophyll a and chlorophyll b content.

4.8. Statistical analysis

The data were analysed using analysis of variance (ANOVA) with SPSS 18.0 statistical software (SPSS, Inc., Chicago, IL, USA), and significant differences between the treatments were investigated using Tukey's multiple comparison test at the $P < 0.05$ significance level.

5. Conclusions

The present study found that solanesol is abundant in tobacco leaves and provides a starting point for further research regarding solanesol biosynthesis genes in tobacco plants. Here, six *DXS*, two *DXR*, two *IspD*, four *IspE*, two *IspF*, four *IspG*, two *IspH*, six *IPI*, and two *SPS* genes were identified to be involved in solanesol biosynthesis. Furthermore, the two *N. tabacum* SPS (NtSPS1 and NtSPS2) were highly homologous with SPS enzymes from other solanaceous plant species. In addition, the solanesol contents of three organs, and leaves from four growing stages, corresponded with the distribution of chlorophyll. Our findings provide a comprehensive evaluation of the correlation between the expression of different biosynthetic genes and the accumulation of solanesol in tobacco.

Acknowledgments: We acknowledge the financial support from the Agricultural Science and Technology Innovation Program (No. ASTIP-TRIC05), the Special Fund for Agro-Scientific Research in the Public Interest of China (No. 201203091) and the Central Public-interest Scientific Institution Basal Research Fund.

Author Contributions: N.Y. and Y.L. conceived, designed and performed the experiments. N.Y., H.Z., Z.Z., J.S., M.P.T., Y.D., X.L., and Y.L. analysed the data. N.Y. and Y.L. wrote the paper.
Conflicts of Interest: The authors declare no conflicts of interest.

References

1. Campbell, R.; Freitag, S.; Bryan, G.J.; Stewart, D.; Taylor, M.A. Environmental and genetic factors associated with solanesol accumulation in potato leaves. *Front. Plant Sci.* **2016**, *7*, 1263.
2. Parmar, S.S.; Jaiwal, A.; Dhankher, O.P.; Jaiwal, P.K. Coenzyme Q_{10} production in plants: current status and future prospects. *Crit. Rev. Biotechnol.* **2015**, *35*, 152–164.
3. Yan, N.; Liu, Y.; Gong, D.; Du, Y.; Zhang, H.; Zhang, Z. Solanesol：a review of its resources, derivatives, bioactivities, medicinal applications, and biosynthesis. *Phytochem. Rev.* **2015**, *14*, 403–417.
4. Bentinger, M.; Tekle, M.; Dallner, G. Coenzyme Q--biosynthesis and functions. *Biochem. Bioph. Res. Co.* **2010**, *396*, 74–79.
5. Sarmiento, A.; Diaz-Castro, J.; Pulido-Moran, M.; Kajarabille, N.; Guisado, R.; Ochoa, J.J. Coenzyme Q_{10} supplementation and exercise in healthy humans: a systematic review. *Curr. Drug Metab.* **2016**, *17*, 345–358.
6. Mezawa, M.; Takemoto, M.; Onishi, S.; Ishibashi, R.; Ishikawa, T.; Yamaga, M.; Fujimoto, M.; Okabe, E.; He, P.; Kobayashi, K.; Yokote, K. The reduced form of coenzyme Q_{10} improves glycemic control in patients with type 2 diabetes: An open label pilot study. *BioFactors* **2012**, *38*, 416–421.
7. Hamidi, M.S.; Gajic-Veljanoski, O.; Cheung, A.M. Vitamin K and bone health. *J. Clin. Densitom.* **2013**, *16*, 409–413.
8. Enokida, H.; Gotanda, T.; Oku, S.; Imazono, Y.; Kubo, H.; Hanada, T.; Suzuki, S.; Inomata, K.; Kishiye, T.; Tahara, Y.; Nishiyama, K.; Nakagawa, M. Reversal of P-glycoprotein-mediated paclitaxel resistance by new synthetic isoprenoids in human bladder cancer cell line. *Jap. J. Cancer Res.* **2002**, *93*, 1037–1046.
9. Sidorova, T.A.; Nigmatov, A.G.; Kakpakova, E.S.; Stavrovskaya, A.A.; Gerassimova, G.K.; Shtil, A.A.; Serebryakov, E.P. Effects of isoprenoid analogues of SDB-ethylenediamine on multidrug resistant tumor cells alone and in combination with chemotherapeutic drugs. *J. Med. Chem.* **2002**, *45*, 5330–5339.
10. Yao, X.; Bai, Q.; Yan, D.; Li, G.; Lü, C.; Xu, H. Solanesol protects human hepatic L02 cells from ethanol-induced oxidative injury via upregulation of HO-1 and Hsp70. *Toxicol. in Vitro* **2015**, *29*, 600–608.
11. Roe, S.J.; Oldfield, M.F.; Geach, N.; Baxter, A. A convergent stereocontrolled synthesis of [3-^{14}C]solanesol. *J. Labelled Compound. Rad.* **2013**, *56*, 485–491.
12. Taylor, M.A.; Fraser, P.D. Solanesol: Added value from *Solanaceous* waste. *Phytochemistry* **2011**, *72*, 1323–1327.
13. Zhou, H.Y.; Liu, C.Z. Rapid determination of solanesol in tobacco by highperformance liquid chromatography with evaporative light scattering detection following microwave-assisted extraction. *J. Chromatogr. B* **2006**, *835*, 119–122.
14. Fukusaki, E.; Takeno, S.; Bamba, T.; Okumoto, H.; Katto, H.; Kajiyami, S.; Kobayashi, A. Biosynthetic pathway for the C45 polyprenol, solanesol, in tobacco. *Biosci. Biotech. Bioch.* **2004**, *68*, 1988–1990.
15. Bajda, A.; Konopka-Postupolska, D.; Krzymowska, M.; Hennig, J.; Skorupinska-Tudek, K.; Surmacz, L.; Wojcik, J.; Matysiak, Z.; Chojnacki, T.; Skorzynska-Polit, E.; Drazkiewicz, M.; Patrzylas, P.; Tomaszewska, M.; Kania, M.; Swist, M.; Danikiewicz, W.; Piotrowska, W.; Swiezewska, E. Role of polyisoprenoids in tobacco resistance against biotic stresses. *Physiol. Plantarum* **2009**, *135*, 351–364.
16. Walter, M.H.; Hans, J.; Strack, D. Two distantly related genes encoding 1-deoxy-d-xylulose 5-phosphate synthases: differential regulation in shoots and apocarotenoid-accumulating mycorrhizal roots. *Plant J.* **2002**, *31*, 243–254.
17. Estévez, J.M.; Cantero, A.; Reindl, A.; Reichler, S.; León, P. 1-Deoxy-D-xylulose-5-phosphate synthase, a limiting enzyme for plastidic isoprenoid biosynthesis in plants. *J. Biol. Chem.* **2001**, *276*, 22901–22909.
18. Muñoz-Bertomeu, J.; Arrillaga, I.; Ros, R.; Segura, J. Up-regulation of 1-deoxy-D-xylulose-5-phosphate synthase enhances production of essential oils in transgenic spike lavender. *Plant Physiol.* **2006**, *142*, 890–900.
19. Zhang, H.; Niu, D.; Wang, J.; Zhang, S.; Yang, Y.; Jia, H.; Cui, H. Engineering a platform for photosynthetic pigment, hormone and cembrane-related diterpenoid production in *Nicotiana tabacum*. *Plant Cell Physiol.* **2015**, *56*, 2125–2138.
20. Carretero-Paulet, L.; Cairó, A.; Botella-Pavía, P.; Besumbes, O.; Campos, N.; Boronat, A.; Rodríguez-Concepción, M. Enhanced flux through the methylerythritol 4-phosphate pathway in *Arabidopsis* plants overexpressing deoxyxylulose 5-phosphate reductoisomerase. *Plant Mol. Biol.* **2006**, *62*, 683–695.

21. Hasunuma, T.; Takeno, S.; Hayashi, S.; Okumoto, H.; Katto, H.; Kajiyami, S.; Kobayashi, A. Overexpression of 1-deoxy-Dxylulose-5-phosphate reductoisomerase gene in chloroplast contributes to increment of isoprenoid production. *J. Biosci. Bioeng.* **2008**, *105*, 518–526.
22. Sabater-Jara, A.B.; Souliman-Youssef, S.; Novo-Uzal, E.; Almagro, L.; Belchı-Navarro, S.; Pedreno, M.A. Biotechnological approaches to enhance the biosynthesis of ginkgolides and bilobalide in *Ginkgo biloba*. *Phytochem. Rev.* **2013**, *12*, 191–205.
23. Hsieh, M.; Chang, C.; Hsu, S.; Chen, J. Chloroplast localization of methylerythritol 4-phosphate pathway enzymes and regulation of mitochondrial genes in ispD and ispE albino mutants in *Arabidopsis*. *Plant Mol. Biol.* **2008**, *66*, 663–673.
24. Kim, S.M.; Kuzuyama, T.; Chang, Y.J.; Kim, S.U. Cloning and characterization of 2-C-methyl-D: -erythritol 2,4-cyclodiphosphate synthase (MECS) gene from *Ginkgo biloba*. *Plant Cell Rep.* **2006**, *25*, 829–885.
25. Gao, S.; Lin, J.; Liu, X.; Deng, Z.; Li, Y.; Sun, X.; Tang, K. Molecular cloning, characterization and functional analysis of a 2C-methyl-D-erythritol 2, 4-cyclodiphosphate synthase gene from *Ginkgo biloba*. *J. Biochem. Mol. Biol.* **2006**, *39*, 502–510.
26. Lu, J.; Wu, W.; Cao, S.; Zhao, H.; Zeng, H.; Lin, L.; Sun, X.; Tang, K. Molecular cloning and characterization of 1-hydroxy-2-methyl-2-(E)-butenyl-4-diphosphate reductase gene from *Ginkgo biloba*. *Mol. Biol. Rep.* **2008**, *35*, 413–420.
27. Kim, S.M.; Kuzuyama, T.; Kobayashi, A.; Sando, T.; Chang, Y.J.; Kim, S.U. 1-Hydroxy-2-methyl-2-(E)-butenyl 4-diphosphate reductase (IDS) is encoded by multicopy genes in gymnosperms *Ginkgo biloba* and *Pinus taeda*. *Planta* **2008**, *227*, 287–298.
28. Berthelot, K.; Estevez, Y.; Deffieux, A.; Peruch, F. Isopentenyl diphosphate isomerase: A checkpoint to isoprenoid biosynthesis. *Biochimie* **2012**, *94*, 1621–1634.
29. Nakamura, A.; Shimada, H.; Masuda, T.; Ohta, H.; Takamiya, K. Two distinct isopentenyl diphosphate isomerases in cytosol and plastid are differentially induced by environmental stresses in tobacco. *FEBS Lett.* **2001**, *506*, 61–64.
30. Sun, J.; Zhang, Y.Y.; Liu, H.; Zou, Z.; Zhang, C.J.; Li, H. X.; Ye, Z.B. A novel cytoplasmic isopentenyl diphosphate isomerase gene from tomato (*Solanum lycopersicum*): cloning, expression, and color complementation. *Plant Mol. Biol. Rep.* **2010**, *28*, 473–480.
31. Block, A.; Fristedt, R.; Rogers, S.; Kumar, J.; Barnes, B.; Barnes, J.; Elowsky, C.G.; Wamboldt, Y.; Mackenzie, S.A.; Redding, K.; Merchant, S.S.; Basset, G.J. Functional modeling identifies paralogous solanesyl-diphosphate synthases that assemble the side chain of plastoquinone-9 in plastids. *J. Biol. Chem.* **2013**, *288*, 27594–27606.
32. Hirooka, K.; Izumi, Y.; An, C.I.; Nakazawa, Y.; Fukusaki, E.; Kobayashi, A. Functional analysis of two solanesyl diphosphate synthases from *Arabidopsis thaliana*. *Biosci. Biotech.Bioch.* **2005**, *69*, 592–601.
33. Jun, L.; Saiki, R.; Tatsumi, K.; Nakagawa, T.; Kawamukai, M. Identification and subcellular localization of two solanesyl diphosphate synthases from *Arabidopsis thaliana*. *Plant Cell Physiol.* **2004**, *45*, 1882–1888.
34. Phatthiya, A.; Takahashi, S.; Chareonthiphakorn, N.; Koyama, T.; Wititsuwannakul, D.; Wititsuwannakul, R. Cloning and expression of the gene encoding solanesyl diphosphate synthase from *Hevea brasiliensis*. *Plant Sci.* **2007**, *172*, 824–831.
35. Ohara, K.; Sasaki, K.; Yazaki, K. Two solanesyl diphosphate synthases with different subcellular localizations and their respective physiological roles in *Oryza sativa*. *J. Exp. Bot.* **2010**, *61*, 2683–2692.
36. Jones, M.O.; Perez-Fons, L.; Robertson, F.P.; Bramley, P.M.; Fraser, P.D. Functional characterization of long-chain prenyl diphosphate synthases from tomato. *Biochem. J.* **2013**, *449*, 729–740.
37. Tamura, K.; Peterson, D.; Peterson, N.; Stecher, G.; Nei, M.; Kumar, S. MEGA5: molecular evolutionary genetics analysis using maximum likelihood, evolutionary distance, and maximum parsimony methods. *Mol. Biol. Evol.* **2011**, *28*, 2731–2739.
38. Wang, L.J.; Fang, X.; Yang, C.Q.; Li, J.X.; Chen, X.Y. Biosynthesis and regulation of secondary terpenoid metabolism in plants. *Scientia Sinica Vitae* **2013**, *43*, 1030–1046.
39. Grabherr, M.G.; Haas, B.J.; Yassour, M.; Levin, J.; Thompson, D.A.; Amit, I.; Adiconis, X.; Fan, L.; Raychowdhury, R.; Zeng, Q.; Chen, Z.; Mauceli, E.; Hacohen, N.; Gnirke, A.; Rhind, N.; di Palma, F.; Birren, B.W.; Nusbaum, C.; Lindblad-Toh, K.; Friedman, N.; Regev, A. Full-length transcriptome assembly from RNA-seq data without a reference genome. *Nat. Biotechnol.* **2011**, *29*, 644–652.

40. Mortazavi, A.; Williams, B.A.; McCue, K.; Schaeffer, L.; Wold, B. Mapping and quantifying mammalian transcriptomes by RNA-Seq. *Nat. Methods* **2008**, *5*, 621–628.

41. Yan, N.; Xu, X.F.; Wang, Z.D.; Huang, J.Z.; Guo, D.P. Interactive effects of temperature and light intensity on photosynthesis and antioxidant enzyme activity in *Zizania latifolia* Turcz. plants. *Photosynthetica* **2013**, *51*, 127–138.